JACS
JOURNAL OF THE AMERICAN CHEMICAL SOCIETY

COMMUNICATION

pubs.acs.org/JACS

Light-Induced Selective Deposition of Metals on Gold-Tipped CdSe-Seeded CdS Nanorods

Xinheng Li,[†] Jie Lian,[†] Ming Lin, and Yinthai Chan*

Department of Chemistry, National University of Singapore, 3 Science Drive 3, Singapore 117543, and Institute of Materials Research and Engineering, A*STAR, 3 Research Link, Singapore 117602

Supporting Information

ABSTRACT: We introduce a facile approach for the selective deposition of metals on Au-tipped CdSe-seeded CdS nanorods that exploits the transfer of electrons from CdS to the Au tips upon UV excitation. This light-induced deposition method was used for the deposition of Pd under mild conditions, which produced a Pd/Au alloyed tip while preserving the rest of the semiconductor nanoarchitecture. The highly site-selective deposition method was extended to the deposition of Fe, yielding monodispersed, structurally complex Au core/Fe_xO_y hollow shell-tipped semiconductor nanorods. These structurally well-defined rods were found to exhibit magnetic functionality. The synthetic strategies described in this work expand on the range of metals that can be deposited on heterostructured semiconductor nanorods, opening up new avenues for the hierarchical buildup of structural complexity and therefore multifunctionality in nanoparticles.

Heterostructured hybrid metal−semiconductor nanostructures are greatly desired because they potentially combine optical, electronic, and/or magnetic properties within a single architecture and show promise in applications such as photocatalysis[1] and directed self-assembly.[2a−2c] To date, numerous examples of such structures have been reported, including Co−CdSe,[3a] Co−CdSe/CdS,[3b] Co−TiO_2,[3c] Au−CdSe,[3d] Au−CdSe/CdS,[3e] Pt−CdS,[3f] and Au−PbS,[3g] to name a few. A common strategy for deriving such structures is first to synthesize the semiconductor nanoparticle and then to proceed with heterogeneous nucleation and growth of the metal counterpart via a relatively mild deposition process. Depending upon the affinity of the metal for the semiconductor surface, minimizing homogeneous nucleation of the metal precursor and/or Ostwald ripening of the semiconductor particle during the deposition process can be difficult, which limits the range of metals that can be deposited onto a given semiconductor. We report here an alternative approach using as the starting structure metal-tipped semiconductor nanorods (NRs), where the metal tip serves as the heterogeneous nucleation site for subsequent deposition of a different metal. Using Au-tipped CdSe-seeded CdS NRs as our exemplary model, we have shown that Pd can selectively be deposited onto the Au tips of the NRs under relatively mild reaction conditions, thus preserving the size and shape monodispersity of the starting rods. We have extended this strategy to the deposition of Fe, successfully obtaining core−shell Au−Fe_xO_y-tipped CdSe-seeded CdS nanoheterostructures that also exhibit magnetic functionality.

Among the various anisotropic shapes of metal−semiconductor nanostructures that have been fabricated, metal-tipped semiconductor NRs are particularly interesting because the long axis of the rod naturally provides a directed path for charge transport,[4] and it has been shown in the case of Au-tipped CdSe-seeded CdS NRs under UV excitation that electrons from the CdS rodlike shell migrate to the Au tip, leaving holes behind. This in turn was found to facilitate the growth of large Au domains at the rod tips via a photoreduction process.[5] We surmised that as a result of the transfer of electrons to the Au tip, redox processes would be enhanced at its surface, thus potentially providing a strategy to expand the range of metals that can be deposited at the NR tips under mild reducing conditions. In order to investigate this hypothesis, CdSe-seeded CdS NRs bearing Au nanoparticles at their tips with matchstick [Figure S1A in the Supporting Information (SI)] and dumbbell-like (Figure S2) structures were synthesized according to a previously established method in which growth of an additional Au tip at the opposite end of the rod may be facilitated by an increase in the concentration of Au precursor added.[3e] Briefly, the synthesis of Au-tipped CdSe-seeded CdS NRs with matchsticklike geometry yielded monodisperse 30 nm long NRs with 2.75 nm diameter cores and Au tips with a diameter of ∼1.4 nm. The processed Au−CdSe/CdS NRs were dispersed in a toluene mixture containing octadecylphosphonic acid (ODPA) and exposed to a reddish clear solution of $PdCl_2$, tetraoctylammonium bromide (TOAB), and dodecylamine (DDA) in toluene (see the SI for details). Ethanol was added as a hole scavenger, and the entire reaction proceeded at room temperature under UV irradiation for ∼1 h.

Figure 1A shows a representative transmission electron microscopy (TEM) image of matchsticklike 1.4 nm diameter Au-tipped NRs after Pd deposition, which resulted in an increase in average diameter to ∼4.3 nm with Pd deposition occurring solely at the Au tip. No free particles of Pd were observed, signaling successful suppression of homogeneous nucleation events with respect to Pd. Continued growth of the Pd−Au spherical tip resulted in a progressive loss of absorption features in comparison with the starting Au-tipped CdSe-seeded CdS nanorods, as shown by UV−vis measurements (Figure S3). High-angle annular dark-field scanning TEM (HAADF-STEM) data for a typical rod (Figure 1B) suggested a homogeneous material distribution at the bulbous tip, while analysis by energy-dispersive X-ray (EDX) line scan (Figure 1C) indicated the presence of

Received: August 24, 2010
Published: December 21, 2010

ACS Publications © 2010 American Chemical Society

dx.doi.org/10.1021/ja1076603 | J. Am. Chem. Soc. 2011, 133, 672–675

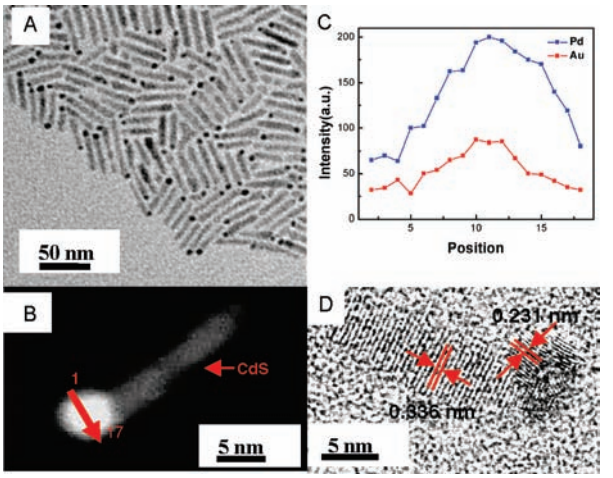

Figure 1. (A) TEM image of Pd−Au-tipped CdSe-seeded CdS nanorod matchsticklike structures. (B) HAADF-STEM image of a typical rod, showing a homogeneous material composition at the spherical tip. The darker region within the rod is ascribed to the CdSe seed. (C) Corresponding EDX line scan across the spherical tip of the matchstick structure using scan steps of 0.3 nm. (D) HRTEM image of a Pd−Au−CdSe-seeded CdS rod. Discernible lattice spacings of 0.231 and 0.336 nm are attributed to the PdAu {111} plane and CdS {002} plane, respectively.

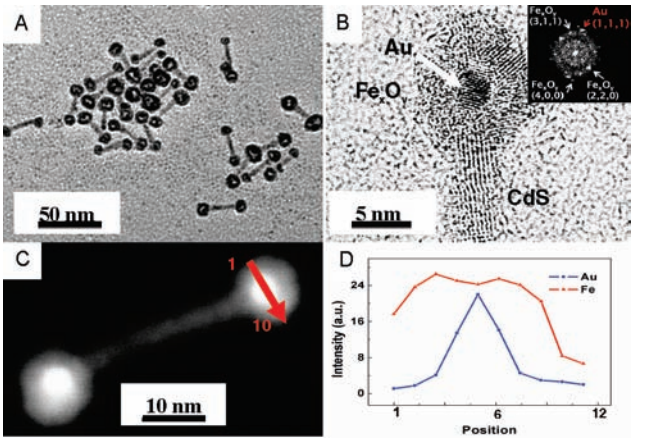

Figure 2. (A) TEM image of ∼2.8 nm diameter core Au nanoparticles with a ∼3.3 nm thick hollow shell of Fe_xO_y exclusively at the tips of 29 nm long CdSe-seeded CdS semiconductor nanorods. (B) HRTEM image of part of the core−shell-tipped rod. The inset is an FFT image of the spherical tip region. (C) HAADF-STEM image of a typical core−shell rod, showing three distinct materials within the same structure. (D) EDX line scan of the spherical tip in the direction of the red arrow shown in (C).

both Pd and Au with similar distribution trends across the tip and a relatively consistent intensity ratio of between ∼2:1 and 3:1. These measurements collectively suggested the formation of a random alloy of Au and Pd, which is surprising in view of the fact that seeded growth under such mild reducing conditions is expected to yield core−shell or dimeric structures.[6a,6b] This may be attributed to the small size of the Au seed, which can undergo spontaneous alloying when exposed to metallic atoms such as Cu.[7] Such a tendency to form alloyed structures was also previously observed in Au−Pd nanoparticles with diameters of less than 5 nm, although in that work, nucleation and growth of the particle was proposed to take place heterogeneously via a Pd seed.[8] It should be noted that in the absence of the Pd precursor, Au-tipped rods under UV exposure did not show any appreciable increase in size, indicating that Ostwald ripening effects under the experimental conditions we employed were insignificant and that the increase in the tip diameter could be ascribed mainly to the addition of Pd. The high-resolution TEM (HRTEM) image in Figure 1D revealed a strongly discernible lattice spacing of 0.231 nm, which lies between the spacings of 0.235 nm for Au {111} and 0.225 nm for Pd {111}, further substantiating the notion that the spherical tip is an alloy of Pd and Au and not a Au core enveloped within a Pd shell. It should be noted that it would be possible to obtain a more exact determination of the tip composition via the use of X-ray absorption spectroscopy,[9] but we were unable to obtain access to such techniques for this present work.

Our control experiments with free gold nanoparticles (Figure S1B−D) or bare CdSe-seeded CdS nanorods (Figure S1E) alone under UV excitation as well as Au-tipped rods without UV illumination (Figure S1F) did not result in any observable Pd deposition. While a quantitative evaluation of the effects of the intensity of the UV excitation on the growth kinetics of the alloyed tip was not pursued in this work, a crude comparison between the excitation at a fixed distance from a hand-held UV lamp (4 W, λ_{exc} = 365 nm) and a UV reactor source (350 W, λ_{exc} = 350 nm) revealed much faster tip growth in the latter. Appropriate control experiments were performed to ensure that the accelerated growth under higher excitation intensity was not simply due to thermal effects, further lending confidence that the reduction and subsequent deposition of the Pd precursor at the Au tip was mediated via a photochemical process and not other irradiation-free mechanisms such as galvanic replacement.[10a,10b]

Our success with Pd deposition prompted us to extend the strategy to other metals that could potentially confer additional functionality. Iron was selected as a choice material because of the fact that it can exhibit magnetic properties even upon oxidation. The deposition of Fe was carried out on monodispersed dumbbell-like Au−CdSe/CdS nanorods with lengths of ∼29 nm and an average Au tip diameter of ∼2.8 nm. Briefly, processed Au-tipped rods dispersed in a mixture of octadecene, oleylamine, and oleic acid were first exposed to $Fe(CO)_5$ in an inert atmosphere at 95 °C under UV excitation and then allowed to oxidize in air. In this case, photoreduction was expected to take place via an iron oleate precursor, which forms readily from the reaction between oleic acid and $Fe(CO)_5$.[11] The resulting nanrods are depicted in Figure 2A, which is a representative TEM image of CdSe-seeded CdS nanorods featuring Au−Fe_xO_y core−hollow shell structures grown exclusively on the Au tips at the two ends of the nanorods. The high selectivity and yield of Fe growth on sites where only Au is present not only highlights the necessity of the latter material as a host substrate (as in the case with Pd deposition) but also demonstrates the ability to controllably produce hierarchically complex nanostructures of potentially expanded functionality. Measurements by HRTEM, as illustrated in Figure 2B, showed the existence of a polycrystalline Fe_xO_y shell around the Au core. Fast Fourier Transform (FFT) analysis of the spherical tip revealed the existence of planes corresponding to those of Au, γ-Fe_2O_3, and/or Fe_3O_4. Selected-area electron diffraction (SAED) measurements also allowed us to exclude the existence of the α-Fe_2O_3 phase, while electron energy loss spectroscopy (EELS) analysis suggested that the shell was primarily Fe_3O_4 with slight oxidation to γ-Fe_2O_3 (see the SI). While the HAADF-STEM image in Figure 2C provided further evidence for the Au core−Fe_xO_y shell configuration, EDX line scans across the tip (Figure 2D) showed a compositional distribution of Au and Fe consistent with a core−shell

dx.doi.org/10.1021/ja1076603 |J. Am. Chem. Soc. 2011, 133, 672–675

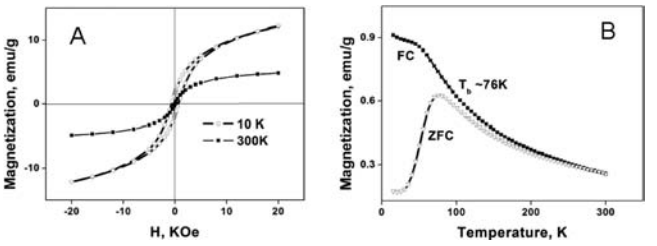

Figure 3. SQUID measurements of Au core−hollow Fe_xO_y shell-tipped CdSe-seeded CdS nanorods. (A) Field-dependent magnetization curves of the sample at (○) 10 and (■) 300 K. (B) Temperature-dependent magnetization of the sample under (■) field-cooled (FC) and (▽) zero-field-cooled (ZFC) conditions. The blocking temperature is $T_b \approx 76$ K.

structure. The formation of the polycrystalline hollow shell structure may be attributed to vacancies created by the outward diffusion of Fe during the oxidation process via the Kirkendall effect, as previously reported by Shevchenko et al.[11] for spherical gold−iron oxide core−shell nanoparticles. Control experiments using free Au nanoparticles, bare CdS nanorods under UV excitation, and Au-tipped rods without UV irradiation resulted in homogeneous nucleation of very small particles of Fe at high precursor concentrations, whereas site-selective heterogeneous nucleation was not detected at any concentration of Fe precursor used (see the SI). It should be noted that at temperatures above 160 °C in the absence of UV light, selective growth of the Fe_xO_y hollow shell at the Au tips could be obtained, but the majority of rods were found to have coalesced via the Au tips, similar to what was reported in ref 10. The use of UV excitation allowed for a much milder temperature of 95 °C to be used, resulting in almost no coalescence between the Au tips of rods. These observations, along with those of the Pd system, corroborate our hypothesis that electron transfer from the semiconductor rod to the Au tips enhances the deposition of other metals at their surface via a photoinduced process.

The magnetic properties of the newly synthesized heterostructures were investigated by superconducting quantum interference device (SQUID) magnetometry. Figure 3A shows the magnetization as a function of applied magnetic field at two different temperatures. A hysteresis loop was clearly seen at 10 K but disappeared when the measurements were performed at 300 K, indicating that the Au−Fe_xO_y core−hollow shell-tipped nanorods exhibit superparamagnetic behavior. The saturation magnetization (M_s) of 16 emu/g is significantly lower than those of bulk γ-Fe_2O_3 (74 emu/g) and Fe_3O_4 (80−84 emu/g) and may be attributed to nanoscale-related surface effects such as canted and/or disordered spins associated with dangling bonds,[12a,12b] which typically require very high fields in order to achieve saturation.[12c] This is certainly applicable in our system, as reflected by the lack of magnetization saturation at 10 K even at fields of 20 KOe. Additionally, demagnetization effects from the CdS rod in intimate contact with the hollow shell, as observed previously with Fe_xO_y-tipped TiO_2 nanorods,[13] may explain the comparably lower M_s relative to those of isolated spherical core−shell Au−Fe_xO_y nanoparticles.[11] The decline in M_s from 10 to 300 K, which is exacerbated as the particle size decreases,[14] is reasonable given the relatively thin Fe_xO_y shell (~3.3 nm thick) on the small-sized Au cores (~2.8 nm diameter) obtained. The results of temperature-dependent zero-field-cooled (ZFC) and field-cooled (FC) magnetization measurements are given in Figure 3B. From the peak magnetization of the ZFC curve, a blocking temperature (T_b) of ~76 K was obtained. Below the blocking temperature, the core−shell-tipped rods displayed ferromagnetic behavior, as seen from the FC curve.

In summary, we have reported a photochemical approach for the selective deposition of metals onto core-seeded semiconductor nanorods by using an existing metal tip as the deposition site. By exploiting the fact that in Au-tipped CdSe-seeded CdS nanorods under UV excitation, electrons from CdS migrate to the Au tips, we achieved deposition of metals such as Pd and Fe at the rod apexes. The deposition of these metals onto Cd chalcogenide nanorods is, to the best of our knowledge, unprecedented. The relatively mild UV-excitation-assisted metal deposition process did not produce any detrimental effects on the size or morphology of the semiconductor rods, attesting to its utility as a facile strategy for expanding the range of metals and potential functionalities that can be introduced to the heterostructured semiconductor nanorods. In this work, the introduction of Pd to form Pd−Au alloyed tips may offer enhanced catalytic properties, while the introduction of Fe to form Au core−Fe_xO_y hollow shell tips imparted magnetic functionality. Facilitating the hierarchical buildup of complex metal−semiconductor nanocomposites, as exemplified in this work, will undoubtedly open up avenues for new or enhanced applications in catalysis and optoelectronics.

■ ASSOCIATED CONTENT

Supporting Information. Synthesis details, UV−vis absorption spectra, SAED data, EELS data, and control experiments for the deposition of Pd and Fe_xO_y. This material is available free of charge via the Internet at http://pubs.acs.org.

■ AUTHOR INFORMATION

Corresponding Author
chmchany@nus.edu.sg

Author Contributions
[†]These authors contributed equally.

■ ACKNOWLEDGMENT

This work was supported by NUS Startup Grant WBS-R143-000-367-133. We thank Professor George Zhao and Dr. Zhigang Xiong in the Department of Chemical and Biomolecular Engineering, National University of Singapore, for their kind assistance in the use of UV reactors.

■ REFERENCES

(1) Costi, R.; Saunders, A. E.; Salant, A.; Banin, U. *Nano Lett.* **2008,** *8,* 637.

(2) (a) Zhao, N.; Liu, K.; Greener, J.; Nie, Z.; Kumacheva, E. *Nano Lett.* **2009,** *9,* 3077. (b) Salant, A.; Amitay-Sadovsky, E.; Banin, U. *J. Am. Chem. Soc.* **2006,** *128,* 10006. (c) Figuerola, A.; Huis, M. V.; Zanella, M.; Genovese, A.; Marras, S.; Falqui, A.; Zandberg, H. W.; Manna, L. *Nano Lett.* **2010,** *10,* 3028.

(3) (a) Maynadié, J.; Salant, A.; Falqui, A.; Respaud, M.; Shaviv, E.; Banin, U.; Soulantica, K.; Chaudret, B. *Angew. Chem., Int. Ed.* **2009,** *48,* 1814. (b) Deka, S.; Falqui, A.; Bertoni, G.; Sangregorio, C.; Poneti, G.; Morello, G.; De Giorgi, M.; Giannini, C.; Cingolani, R.; Manna, L.; Cozzoli, P. D. *J. Am. Chem. Soc.* **2009,** *131,* 12817. (c) Casavola, M.; Grillo, V.; Carlino, E.; Giannini, C.; Gozzo, F.; Pinel, E. F.; Garcia, M. A.; Manna, L.; Cingolani, R.; Cozzolli, P. D. *Nano Lett.* **2007,** *7,* 1386. (d) Mokari, T.; Rothenberg, E.; Popov, I.; Costi, R.; Banin, U. *Science* **2004,**

304, 1787. (e) Chakrabortty, S.; Yang, J. A.; Tan, Y. M.; Mishra, N.; Chan, Y. *Angew. Chem., Int. Ed.* **2010,** *49*, 2888. (f) Habas, S. E.; Yang, P. D.; Mokari, T. *J. Am. Chem. Soc.* **2008,** *130*, 3294. (g) Yang, J.; Elim, H. I.; Zhang, Q.; Lee, J. Y.; Ji, W. *J. Am. Chem. Soc.* **2006,** *128*, 11921.

(4) Huynh, W. U.; Dittmer, J. J.; Alivisatos, A. P. *Science* **2002,** *295*, 2425.

(5) Carbone, L.; Jakab, A.; Khalavka, Y.; Sönnichsen, C. *Nano Lett.* **2009,** *9*, 3710.

(6) (a) Xu, J.; White, T.; Li, P.; He, C.; Yu, J.; Yuan, W.; Han, Y.-F. *J. Am. Chem. Soc.* **2010,** *132*, 10398. (b) Fan, F.-R.; Liu, D.-Y.; Wu, W.-F.; Duan, S.; Xie, Z.-X.; Jiang, Z.-Y.; Tian, Z.-Q. *J. Am. Chem. Soc.* **2008,** *130*, 6949.

(7) Yasuda, H.; Mori, H.; Komatu, M.; Takeda, K. *J. Appl. Phys.* **1993,** *73*, 1100.

(8) Ferrer, D.; Torres-Castro, A.; Gao, X.; Sepulveda-Guzman, S.; Ortiz-Mendez, U.; Jose-Yacaman, M. *Nano Lett.* **2007,** *7*, 1701.

(9) Yuhas, B. D.; Habas, S. E.; Fakra, S. C.; Mokari, T. *ACS Nano* **2009,** *3*, 3369.

(10) (a) Yang, Y.; Gong, X.; Zeng, H.; Zhang, L.; Zhang, X.; Zou, C.; Huang, S. *J. Phys. Chem. C* **2010,** *114*, 256. (b) Teng, X.; Wang, Q.; Liu, P.; Han, W.; Frenkel, A.; Wen, W.; Marinkovic, N.; Hanson, J. C.; Rodriguez, J. A. *J. Am. Chem. Soc.* **2008,** *130*, 1091.

(11) Shevchenko, E. V.; Bodnarchuk, M. I.; Kovalenko, M. V.; Talapin, D. T.; Smith, R. K.; Aloni, S.; Heiss, W.; Alivisatos, A. P. *Adv. Mater.* **2008,** *20*, 4323.

(12) (a) Park, J.; An, K.; Hwang, Y.; Park, J.-G.; Noh, H.-J.; Kim, J.-Y.; Park, J.-H.; Hwang, N.-M.; Hyeon, T. *Nat. Mater.* **2004,** *3*, 891. (b) Park, J.; Lee, E.; Hwang, N.-M.; Kang, M.; Kim, S. C.; Hwang, Y.; Park, J.-G.; Noh, H.-J.; Kim, J.-Y.; Park, J.-H.; Hyeon, T. *Angew. Chem., Int. Ed.* **2005,** *44*, 2872. (c) Martínez-Boubeta, C.; Simeonidis, K.; Angelakeris, M.; Pazos-Pérez, N.; Giersig, M.; Delimitis, A.; Nalbandian, L.; Alexandrakis, V.; Niarchos, D. *Phys. Rev. B* **2006,** *74*, 054430.

(13) Buonsanti, R.; Grillo, V.; Carlino, E.; Giannini, C.; Gozzo, F.; Garcia-Hernandez, M.; Garcia, M. A.; Cingolani, R.; Cozzoli, P. D. *J. Am. Chem. Soc.* **2010,** *132*, 2437.

(14) Zhang, D.; Klabunde, K. J.; Sorensen, C. M. *Phys. Rev. B* **1998,** *58*, 14167.